Efficient Quadrature Squeezing from Biexcitonic Parametric Gain in Atomically Thin Semiconductors

Emil V. Denning, Andreas Knorr, Florian Katsch, and Marten Richter
Nichtlineare Optik und Quantenelektronik, Institut für Theoretische Physik, Technische Universität Berlin, 10623 Berlin, Germany

(Received 23 February 2022; revised 17 May 2022; accepted 19 July 2022; published 22 August 2022)

Modification of electromagnetic quantum fluctuations in the form of quadrature squeezing is a central quantum resource, which can be generated from nonlinear optical processes. Such a process is facilitated by coherent two-photon excitation of the strongly bound biexciton in atomically thin semiconductors. We show theoretically that interfacing an atomically thin semiconductor with an optical cavity makes it possible to harness this two-photon resonance and use the biexcitonic parametric gain to generate squeezed light with input power an order of magnitude below current state-of-the-art devices with conventional third-order nonlinear materials that rely on far off-resonant nonlinearities. Furthermore, the squeezing bandwidth is found to be in the range of several meV. These results identify atomically thin semiconductors as a promising candidate for on-chip squeezed-light sources.

DOI: 10.1103/PhysRevLett.129.097401

Introduction.—Quadrature-squeezed light is important for many quantum-technological applications, e.g., metrology [1–3], computing [4–7], communication [5,8], and simulation [9–11]. Since its first experimental realization using four-wave mixing in an atomic beam [12], quadrature-squeezed light has been demonstrated in many material platforms, such as second-order nonlinear crystals in free space [13–16] and on integrated chips [17–20], third-order nonlinearities in optical fibers [21–24] and on integrated chips [25–28], single-emitter resonance flourescence [29], and excitons in semiconductors [30–32]; for a comprehensive review, see Ref. [33].

Quadrature squeezing is canonically described through the operator $\exp[(za^2 - za^{\dagger 2})/2]$, which reduces the in-phase quadrature noise of a single mode with photon annihilation operator a by an amount of $\exp(-z)$ [34]. Thus, pairwise photon creation, also known as *parametric gain*, generates quadrature squeezing. Coherent excitation of the Coulomb-bound biexciton in semiconductors enables strong resonant enhancement of pairwise creation of energy quanta [35–37], which can provide parametric gain for quadrature squeezing [38]. This efficient two-photon resonance is absent in conventional off-resonant third-order nonlinear materials such as Si_3N_4 [25–28]. Atomically thin semiconductors are particularly interesting in this context, because of their exceptionally strong Coulomb interaction [39–41] and thus strongly bound biexciton [42,43], owing to reduced dimensionality and dielectric screening [44]. Furthermore, polaritonic microcavities with atomically thin semiconductors have already been experimentally demonstrated on a photonic chip [41,45–48].

In this Letter, we theoretically demonstrate that the biexciton allows generation of broadband quadrature-squeezed light on a photonic chip with very low input power (1–10 mW) an order of magnitude below state-of-the-art devices with conventional third-order nonlinearities [25–28]. We consider a laser-driven planar microcavity coupled to an atomically thin semiconductor [Figs. 1(a) and 1(b)], where two optically generated polaritons are converted into a bound biexciton via the many-body Coulomb interaction [Fig. 1(c)], not present in typical atomic level schemes. When the energy of a lower polariton pair $2E_0^-$ matches that of the bound biexciton $E_{b,-}^{xx}$, the process is strongly resonant, and coherent biexcitons are efficiently excited. The generated biexcitons drive the polariton field by spontaneously breaking into pairs, thus providing parametric gain and squeezing [Fig. 1(d)].

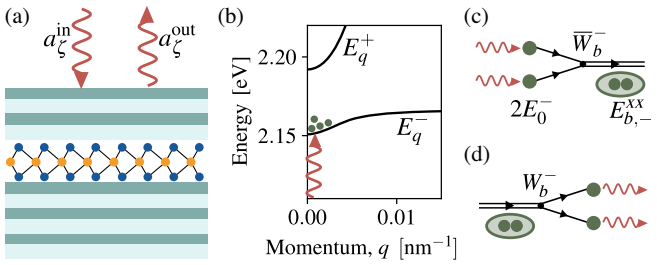

FIG. 1. (a) Atomically thin semiconductor placed in a one-sided planar cavity driven by an optical input field a^{in}. (b) Polariton energy bands with illustration of lower polaritons generated by the input field. (c) Two optically generated lower polaritons can form a bound biexciton via the Coulomb interaction ($\overline{W}_b^-$). When the polariton pair energy ($2E_0^-$) matches the bound biexciton ($E_{b,-}^{xx}$) the process is resonantly enhanced. (d) Bound biexcitons can provide parametric gain by breaking into correlated polariton pairs, which are out-coupled from the cavity as squeezed light.

The analysis of quadrature squeezing in such systems faces two main challenges: first, accounting for the strong correlations generated predominantly by the Coulomb interaction; second, the need for spectral resolution of the squeezing—the key observable in homodyne detection [49,50]—which requires an evaluation of multitime correlation functions. Even though excitonic many-body correlation effects have been studied extensively in semiconductors [51–66], all existing theories of squeezed-light generation in polaritonic microcavities that include spectral resolution are based on mean-field theory and omit Coulomb many-body correlations beyond the Hartree-Fock level [67–71] or considered a phenomenological 1D model [72].

Theory.—The total Hamiltonian of the system is $H = H_0 + H_C$, where H_0 describes free electrons, holes, and photons, and their coupling, and H_C describes Coulomb interactions; external driving is introduced through input-output formalism (see Supplemental Material [73]). The bosonic photon annihilation (creation) operators $a^{(\dagger)}_{\sigma\mathbf{q}}$, with polarization σ and in-plane momentum $\mathbf{q}$ describe the electromagnetic field in the cavity. The fermionic annihilation (creation) operators $c^{(\dagger)}_{\zeta\mathbf{k}}$ and $v^{(\dagger)}_{\zeta\mathbf{k}}$ describe conduction and valence band electrons in the semiconductor, where the compound index $\zeta = (\xi, s)$ labels spin (s) and valley (ξ), and $\mathbf{k}$ is the 2D wave vector.

For atomically thin transition-metal dichalcogenides, the energetically lowest optical transitions appear at the K and K' valleys in the Brillouin zone [cf. Fig. 2(a)]. Because of spin-orbit coupling, right- or left-hand circularly polarized photons ($\sigma = R$ or $\sigma = L$) can excite electron-hole pairs with $\zeta = (K, \uparrow)$ or $\zeta = (K', \downarrow)$ [81–85] [cf. Fig. 2(b)]. Thereby, photon polarization in the circular basis is absorbed into the index ζ to label spin, valley, and polarization as $\zeta \in \{K, K'\}$.

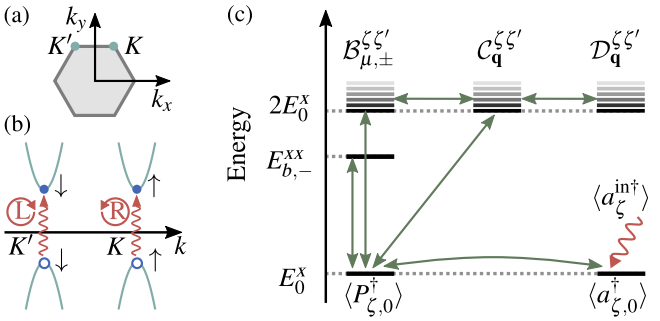

FIG. 2. (a) 2D hexagonal Brillouin zone of atomically thin transition-metal dichalcogenide semiconductors with symmetry points K and K', where direct exciton transitions occur. (b) Circular optical selection rules for the transitions. (c) Energies of single-exciton and single-photon expectation values and multiparticle correlations (here indicated for $E^p_0 = E^x_0$). The arrows visualize the coupling of expectation values in the dynamical evolution.

The cavity photon energy is given by [86,87] $E^p_{\mathbf{q}} = \hbar[\omega^2_{p,0} + (cq/\bar{n})^2]^{1/2}$, where $\omega_{p,0}$ is the resonance frequency of the cavity mode, c is the vacuum speed of light, and $\bar{n}$ is the effective cavity refractive index. The cavity is taken to be one sided with out-coupling rate γ^p.

The $\mathbf{q} = 0$ mode of the cavity field is driven by coherent light with polarization vector $\boldsymbol{\lambda}_{\mathrm{in}}$ in the circular basis. The quantity of interest is the quadrature operator of the cavity field at $\mathbf{q} = 0$, $X(\theta, t) = e^{i\theta}\boldsymbol{\lambda}^T_{\mathrm{out}}\mathbf{a}^\dagger_0(t) + e^{-i\theta}\boldsymbol{\lambda}^{*T}_{\mathrm{out}}\mathbf{a}_0(t)$, where $\mathbf{a}_0 = (a_{K,0}, a_{K',0})^T$ and $\boldsymbol{\lambda}_{\mathrm{out}}$ is the detected polarization vector and the time argument t denotes Heisenberg time evolution. While the absolute squeezing of the intracavity field can be calculated as the variance of $X(\theta, t)$, a more relevant measure is the squeezing of the out-coupled and thus detected field. This is characterized by the squeezing spectrum $\Lambda(\omega, \theta) = 2\sqrt{2\gamma^p}\int_0^\infty d\tau \cos(\omega\tau)\langle :\delta X(\theta, \tau)\delta X(\theta, 0):\rangle$ [50], where $\delta X(\theta, t) \coloneqq X(\theta, t) - \langle X(\theta, t)\rangle$. The symbols $::$ denote normal and time ordering, such that the time argument increase to the right in products $a^\dagger$ and to the left in products of a. The photocurrent noise spectrum of homodyne detection, normalized to the shot-noise level, is given by $1 + \Lambda(\omega, \theta)$, where θ is the homodyne phase [50]. We use the shorthand notation $\Lambda(\omega)$ to denote the squeezing spectrum at the optimal homodyne phase θ giving the lowest value of $\Lambda(\omega, \theta)$.

In the numerical calculations presented in this Letter, we use strictly linear polarization, $\boldsymbol{\lambda}_{\mathrm{in}} = 2^{-1/2}[1, 1]$, since this allows excitation of the bound biexciton [64]. For detection, we consider the copolarized ($\boldsymbol{\lambda}_{\mathrm{out}} = \boldsymbol{\lambda}_{\mathrm{in}}$) and the cross-polarized ($\boldsymbol{\lambda}_{\mathrm{out}} = 2^{-1/2}[1, -1]$) configurations.

Exciton creation operators are introduced by expanding electron-hole pairs on exciton wave functions as $P^{n\dagger}_{\zeta,\mathbf{q}} = \sum_{\mathbf{k}} \phi^n_{\mathbf{k}} c^\dagger_{\zeta\mathbf{k}+\alpha\mathbf{q}} v_{\zeta\mathbf{k}-\beta\mathbf{q}}$, where $\phi^n_{\mathbf{k}}$ is the momentum-space wave function of the nth exciton state obtained from the Wannier equation [88–90] and $\alpha = m_e/(m_e + m_h)$, $\beta = m_h/(m_e + m_h)$ are coefficients defined from the electron (m_e) and hole (m_h) masses. The lowest-energy exciton ($n = 1s$) is separated from the next state by hundreds of meV [81,91]. Because of this large energy gap and assuming excitation in the vicinity of the $1s$ exciton energy, we truncate the electronic pair space to the $1s$ exciton subspace and omit the index n. Within the effective mass approximation, the exciton energy is $E^x_{\mathbf{q}} = E^x_0 + \hbar^2 q^2/[2(m_e + m_h)]$, with E^x_0 the exciton energy for $\mathbf{q} = 0$.

To study the leading nonlinear response, we apply the dynamics-controlled truncation scheme [51,52,55] to expand the equations of motion to third order in the driving field a^{in}_ζ, which corresponds to keeping only terms up to three normal-ordered electron-hole pair or photon operators. In the Supplemental Material, all details of the derivation are described: A closed set of equations is obtained for the zero-momentum exciton and photon expectation values $\langle a^\dagger_{\zeta,0}\rangle$ and $\langle P^\dagger_{\zeta,0}\rangle$, and three types of

correlations [73]. Two-photon correlations are defined as $\mathcal{D}^{\zeta\zeta'}_{\mathbf{q}} := \langle a^\dagger_{\zeta\mathbf{q}} a^\dagger_{\zeta'-\mathbf{q}}\rangle - \langle a^\dagger_{\zeta\mathbf{q}}\rangle\langle a^\dagger_{\zeta'-\mathbf{q}}\rangle$. Electron-hole-photon correlations $\langle a^\dagger_{\zeta,\mathbf{q}} c^\dagger_{\zeta',\mathbf{k}-\alpha\mathbf{q}} v_{\zeta',\mathbf{k}+\beta\mathbf{q}}\rangle^c = \langle a^\dagger_{\zeta,\mathbf{q}} c^\dagger_{\zeta',\mathbf{k}-\alpha\mathbf{q}} v_{\zeta',\mathbf{k}+\beta\mathbf{q}}\rangle - \langle a^\dagger_{\zeta,\mathbf{q}}\rangle\langle c^\dagger_{\zeta',\mathbf{k}-\alpha\mathbf{q}} v_{\zeta',\mathbf{k}+\beta\mathbf{q}}\rangle$ are projected onto the $1s$ exciton wave functions as $\mathcal{C}^{\zeta\zeta'}_{\mathbf{q}} := \sum_{\mathbf{k}} \phi_{\mathbf{k}} \langle a^\dagger_{\zeta,\mathbf{q}} c^\dagger_{\zeta',\mathbf{k}-\alpha\mathbf{q}} v_{\zeta',\mathbf{k}+\beta\mathbf{q}}\rangle^c$.

Two-pair correlations are defined as $\langle c^\dagger_{\zeta\mathbf{k}+\mathbf{q}} v_{\zeta\mathbf{k}} c^\dagger_{\zeta'\mathbf{k}'-\mathbf{q}} v_{\zeta'\mathbf{k}'}\rangle^c := \langle c^\dagger_{\zeta\mathbf{k}+\mathbf{q}} v_{\zeta\mathbf{k}} c^\dagger_{\zeta'\mathbf{k}'-\mathbf{q}} v_{\zeta'\mathbf{k}'}\rangle - \langle c^\dagger_{\zeta\mathbf{k}+\mathbf{q}} v_{\zeta\mathbf{k}}\rangle \times \langle c^\dagger_{\zeta'\mathbf{k}'-\mathbf{q}} v_{\zeta'\mathbf{k}'}\rangle + \langle c^\dagger_{\zeta'\mathbf{k}'-\mathbf{q}} v_{\zeta\mathbf{k}}\rangle\langle c^\dagger_{\zeta\mathbf{k}+\mathbf{q}} v_{\zeta'\mathbf{k}'}\rangle$. These are first projected on the $1s$ exciton wave function and then partitioned into singlet (−) and triplet (+) channels, defining the biexcitonic correlations $\tilde{\mathcal{B}}^{\zeta\zeta'}_{\mathbf{q},\pm}$ through the relation [92]

$$\frac{1}{2}\left(\langle c^\dagger_{\zeta\mathbf{k}+\mathbf{q}} v_{\zeta\mathbf{k}} c^\dagger_{\zeta\mathbf{k}'-\mathbf{q}} v_{\zeta'\mathbf{k}'}\rangle^c \pm \langle c^\dagger_{\zeta'\mathbf{k}+\mathbf{q}} v_{\zeta\mathbf{k}} c^\dagger_{\zeta\mathbf{k}'-\mathbf{q}} v_{\zeta'\mathbf{k}'}\rangle^c\right) =: \phi^*_{\mathbf{k}+\beta\mathbf{q}}\phi^*_{\mathbf{k}'-\beta\mathbf{q}} \tilde{\mathcal{B}}^{\zeta\zeta'}_{\mathbf{q},\pm} \mp \phi^*_{\alpha\mathbf{k}+\beta(\mathbf{k}'-\mathbf{q})}\phi^*_{\beta(\mathbf{k}+\mathbf{q})+\alpha\mathbf{k}'} \tilde{\mathcal{B}}^{\zeta\zeta'}_{\mathbf{k}'-\mathbf{k}-\mathbf{q},\pm}.$$

These correlations have a more involved structure than exciton-photon and two-photon correlations because of the two possibilities of electron-hole pairing. We transform to a diagonalized biexcitonic basis via the wave functions $\Phi^\pm_{\mu\mathbf{q}}$ with eigenenergies $E^{xx}_{\mu,\pm}$ as $\tilde{\mathcal{B}}^{\zeta\zeta'}_{\mathbf{q},\pm} = \sum_\mu \Phi^\pm_{\mu\mathbf{q}} \mathcal{B}^{\zeta\zeta'}_{\mu,\pm}$ [64,73]. For the singlet channel, bound ($\mu = b, E^{xx}_{b,-} < 2E^x_0$) and unbound ($E^{xx}_{\mu,-} > 2E^x_0$) solutions exist, whereas the triplet channel includes only unbound solutions [59]. The unbound solutions constitute a correlated two-exciton scattering continuum.

Phonon-induced broadening of the excitonic and biexcitonic energies is introduced in the equations of motion through the complex energies $\tilde{E}^x_{\mathbf{q}} = E^x_{\mathbf{q}} + i\hbar\gamma^x$, $\tilde{E}^{xx}_{\mu,\pm} = E^{xx}_{\mu,\pm} + 2i\hbar\gamma^x$, with a self-consistent microscopically calculated γ^x [93–97], and we approximate the biexcitonic damping with $2\gamma^x$ [61,62,98]. Similarly, out-coupling from the cavity is introduced as $\tilde{E}^p_{\mathbf{q}} = E^p_{\mathbf{q}} + i\hbar\gamma^p$.

The time evolution of the expectation values in a rotating frame with the drive frequency ω_d reads [55,64,73]:

$$\begin{aligned}
-i\hbar\partial_t\langle a^\dagger_{\zeta,0}\rangle &= (\tilde{E}^p_0 - \hbar\omega_d)\langle a^\dagger_{\zeta,0}\rangle + \Omega_0\langle P^\dagger_{\zeta,0}\rangle + i\hbar\sqrt{2\gamma^p}\langle a^{\mathrm{in}\dagger}_\zeta\rangle,\\
-i\hbar\partial_t\langle P^\dagger_{\zeta,0}\rangle &= (\tilde{E}^x_0 - \hbar\omega_d)\langle P^\dagger_{\zeta,0}\rangle + \Omega_0\langle a^\dagger_{\zeta,0}\rangle - \sum_{\mathbf{q}}\tilde{\Omega}_{\mathbf{q}}(\mathcal{C}^{\zeta\zeta'}_{\mathbf{q}} + \delta_{\mathbf{q},0}\langle a^\dagger_{\zeta,0}\rangle\langle P^\dagger_{\zeta,0}\rangle)\langle P_{\zeta,0}\rangle + W^0|\langle P^\dagger_{\zeta,0}\rangle|^2\langle P^\dagger_{\zeta,0}\rangle + \sum_{\mu\zeta'\pm} W^\pm_\mu \mathcal{B}^{\zeta\zeta'}_{\mu,\pm}\langle P_{\zeta',0}\rangle,\\
-i\hbar\partial_t\mathcal{B}^{\zeta\zeta'}_{\mu,\pm} &= (\tilde{E}^{xx}_{\mu,\pm} - 2\hbar\omega_d)\mathcal{B}^{\zeta\zeta'}_{\mu,\pm} + \frac{1}{2}(1\pm\delta_{\zeta\zeta'})\left\{\bar{W}^\pm_\mu\langle P^\dagger_{\zeta,0}\rangle\langle P^\dagger_{\zeta',0}\rangle + \sum_{\mathbf{q}}[\bar{\Omega}^\pm_{\mu,-\mathbf{q}}\mathcal{C}^{\zeta'\zeta}_{-\mathbf{q}} + \bar{\Omega}^\pm_{\mu,\mathbf{q}}\mathcal{C}^{\zeta\zeta'}_{\mathbf{q}}]\right\},\\
-i\hbar\partial_t\mathcal{C}^{\zeta\zeta'}_{\mathbf{q}} &= (\tilde{E}^p_{\mathbf{q}} + \tilde{E}^x_{\mathbf{q}} - 2\hbar\omega_d)\mathcal{C}^{\zeta\zeta'}_{\mathbf{q}} + \Omega_{\mathbf{q}}\mathcal{D}^{\zeta\zeta'}_{\mathbf{q}} - \frac{1}{2}\delta_{\zeta\zeta'}\tilde{\Omega}_{\mathbf{q}}\langle P^\dagger_{\zeta,0}\rangle^2 + \sum_{\mu\pm}\Omega^\pm_{\mu,\mathbf{q}}\mathcal{B}^{\zeta\zeta'}_{\mu,\pm},\\
-i\hbar\partial_t\mathcal{D}^{\zeta\zeta'}_{\mathbf{q}} &= 2(\tilde{E}^p_{\mathbf{q}} - \hbar\omega_d)\mathcal{D}^{\zeta\zeta'}_{\mathbf{q}} + \Omega_{\mathbf{q}}\mathcal{C}^{\zeta'\zeta}_{-\mathbf{q}} + \Omega_{-\mathbf{q}}\mathcal{C}^{\zeta\zeta'}_{\mathbf{q}}.
\end{aligned} \tag{1}$$

The first term in every equation describes free evolution, and the remaining terms describe couplings as illustrated in Fig. 2(c). For the photon amplitude $\langle a^\dagger_{\zeta,0}\rangle$, the second term describes linear coupling to the exciton with rate Ω_0 (where $2\Omega_0$ is the vacuum Rabi splitting) and the last term is input-field driving through the cavity mode, where the input-field expectation value is related to the input power $\mathcal{P}_{\mathrm{in}}$ and polarization as [99] $\langle \mathbf{a}^{\mathrm{in}\dagger}\rangle = \boldsymbol{\lambda}_{\mathrm{in}}[\mathcal{P}_{\mathrm{in}}/E^p_0]^{1/2}$. For $\langle P^\dagger_{\zeta,0}\rangle$, the second term describes linear coupling to photons. The third term stems from the fermionic substructure of excitons and generates nonlinear saturation of the light-matter interaction due to Pauli blocking $\tilde{\Omega}_{\mathbf{q}}$. The last two terms describe uncorrelated mean-field Coulomb interactions (W^0) and beyond that Coulomb interactions with the biexcitonic correlations ($W^\pm_\mu$).

For the biexcitonic correlations $\mathcal{B}^{\zeta\zeta'}_{\mu,\pm}$, the second term contains Coulomb scattering of uncorrelated excitons ($\overline{W}^\pm_\mu$). For the bound biexciton ($\mu = b$), this corresponds to the process depicted in Fig. 1(c). The third term describes coupling to exciton-photon correlations through the light-matter interaction ($\overline{\Omega}^\pm_{\mu,\mathbf{q}}$). For the exciton-photon correlations $\mathcal{C}^{\zeta\zeta'}_{\mathbf{q}}$, the second term describes linear coupling to two-photon correlations by exchanging an exciton with a photon (Ω_0). The third term describes nonlinear scattering of two uncorrelated excitons ($\tilde{\Omega}_{\mathbf{q}}$), and the last term describes coupling to biexcitonic correlations via optical fields ($\Omega^\pm_{\mu,\mathbf{q}}$). The second and third terms in the equation of motion for two-photon correlations $\mathcal{D}^{\zeta\zeta'}_{\mathbf{q}}$ describe coupling to exciton-photon correlations by exchanging a photon with an exciton through the light-matter coupling Ω_0. All definitions are given in the Supplemental Material [73].

As we will show, the bound biexciton $\mathcal{B}^{\zeta\zeta'}_{b,-}$ is the dominating contribution to the parametric gain as depicted in Fig. 1(d). This effect is absent in conventional third-order nonlinear materials driven far off-resonantly and in two-level systems, which only have Pauli-blocking nonlinearity.

To calculate the squeezing spectrum, we employ a Heisenberg-Langevin approach, where the time-dependent

exciton and photon fluctuation operators $\delta P^{\dagger}_{\zeta,\mathbf{q}} = P^{\dagger}_{\zeta,\mathbf{q}} - \langle P^{\dagger}_{\zeta,\mathbf{q}}\rangle_s$ and $\delta a^{\dagger}_{\zeta,\mathbf{q}} = a^{\dagger}_{\zeta,\mathbf{q}} - \langle a^{\dagger}_{\zeta,\mathbf{q}}\rangle_s$ are defined with respect to the steady-state expectation values of Eq. (1). Multiparticle fluctuations $\delta\mathcal{B}^{\zeta\zeta'}_{\mu,\pm}$, $\delta\mathcal{C}^{\zeta\zeta'}_{\mathbf{q}}$, and $\delta\mathcal{D}^{\zeta\zeta'}_{\mathbf{q}}$ are defined similarly.

Because of the fluctuation-dissipation theorem [99–102], the Heisenberg-Langevin equations are driven by input noise operators for the photons ($\delta a^{\mathrm{in}}_{\zeta}$) and excitons ($\delta P^{\mathrm{in}}_{\zeta,\mathbf{q}}$). Assuming that the fluctuations around their steady-state values are small, we approximate the equations of motion by their linearized form by removing products of fluctuation operators and Fourier transform to obtain

$$
\begin{aligned}
&-(\hbar\omega-\hbar\omega_d+\tilde{E}^p_0)\delta\mathbf{a}^{\dagger}_0(\omega)=\Omega_0\delta\mathbf{P}^{\dagger}_0(\omega)+i\hbar\sqrt{2\gamma^p}\delta\mathbf{a}^{\mathrm{in}\dagger}(\omega),\\
&-[\hbar\omega-\hbar\omega_d+\tilde{E}^x_0+\Sigma(\omega)]\delta\mathbf{P}^{\dagger}_0(\omega)=\mathbf{\Omega}^r_0(\omega)\delta\mathbf{a}^{\dagger}_0(\omega)+\mathbf{\Delta}\delta\mathbf{P}_0(\omega)\\
&+i\hbar\sqrt{2\mathbf{\Gamma}^x(\omega)}\delta\mathbf{P}^{\mathrm{in}\dagger}_0(\omega)+i\hbar\sqrt{2\mathbf{\Gamma}^p(\omega)}\delta\mathbf{a}^{\mathrm{in}\dagger}(\omega),
\end{aligned}
\tag{2}
$$

where bold symbols denote vectors and matrices in the ζ basis. The multiparticle fluctuation equations have been formally solved, leading to the self-energy $\mathbf{\Sigma}$, the renormalized input field couplings $\mathbf{\Gamma}^{x/p}$, and the renormalized coupling $\mathbf{\Omega}^r_0$ (see Supplemental Material [73]). Equations (2) are solved in order to calculate the squeezing spectrum $\Lambda(\omega)$. Importantly, $\mathbf{\Delta}$ in Eq. (2) is the parametric gain that generates squeezing, which arises from the nonlinear response and takes the form

$$
\begin{aligned}
\Delta_{\zeta\zeta'} = {}& \delta_{\zeta,\zeta'}W^0\langle P^{\dagger}_{\zeta,0}\rangle^2+\sum_{\mu\pm}W^{\pm}_{\mu}\mathcal{B}^{\zeta\zeta'}_{\mu\pm}\\
&-\delta_{\zeta,\zeta'}\sum_{\mathbf{q}}\tilde{\Omega}_{\mathbf{q}}[\mathcal{C}^{\zeta\zeta'}_{\mathbf{q}}+\delta_{\mathbf{q},0}\langle a^{\dagger}_{\zeta,0}\rangle\langle P^{\dagger}_{\zeta,0}\rangle].
\end{aligned}
\tag{3}
$$

This quantity, which in Eq. (2) couples $\delta P^{\dagger}_{\zeta,0}$ to the conjugate field $\delta P_{\zeta',0}$, is analogous to the two-photon pump rate in the well-known degenerate parametric amplifier [34]. The three terms contributing to the parametric gain in Eq. (3) are generated by mean-field exciton Coulomb interaction, biexcitonic correlations, and Pauli blocking, respectively.

Results.—Figures 3(a) and 3(b) show the squeezing as the quadrature noise at zero homodyne detection frequency $1+\Lambda(0)$ in the copolarized output as a function of the drive frequency and the exciton-cavity detuning at 10 mW driving power, for *h*-BN–encapsulated monolayer MoS_2, cavity parameters compatible with fabricated devices [45,48,73], and a temperature of 30 K. The phonon-induced exciton dephasing γ^x should be significantly smaller than the photon out-coupling rate γ^p, such that polaritons are coupled out of the cavity before they scatter with phonons, making cryogenic temperatures necessary.

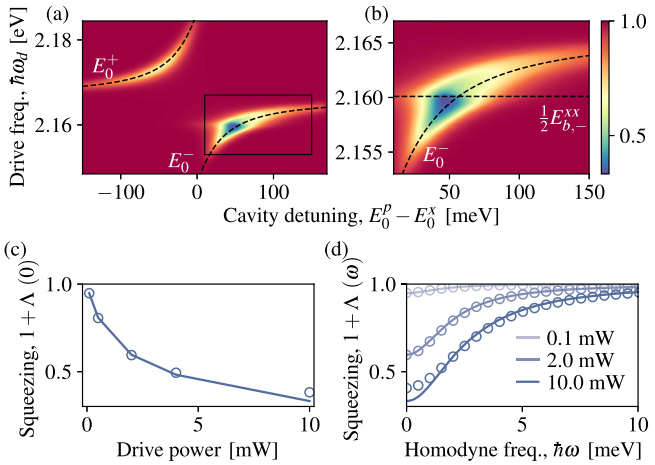

FIG. 3. (a) Squeezing as $1+\Lambda(0)$ in the copolarized output channel versus cavity-exciton detuning and drive frequency for a microcavity with *h*-BN–encapsulated monolayer MoS_2, at 10 mW driving power. Cavity parameters are $\Omega_0 = 20$ meV, $\hbar\gamma^p = 9$ meV. The temperature is 30 K, leading to $\hbar\gamma^x = 0.8$ meV. The laser spot area is 9 μm^2. (b) Enlargement of region indicated by the rectangle in (a). (c) Squeezing at the numerically optimized cavity and driving frequencies versus driving power. Solid lines and open circles signify the copolarized and cross-polarized output channels. (d) Homodyne squeezing spectrum at the optimal driving frequency and cavity detuning.

A value of $1+\Lambda(0)=1$ corresponds to the shot-noise level, i.e., no squeezing, whereas $1+\Lambda(0)=0$ corresponds to complete elimination of noise in one quadrature, i.e., perfect squeezing.

The dominating response is around the polariton energies $E^{\pm}_0 = \frac{1}{2}\{E^p_0+E^x_0 \pm [(E^p_0-E^x_0)^2+4\Omega^2_0]^{1/2}\}$, and a particularly strong squeezing is seen where the lower polariton branch is two-photon resonant with the bound biexciton, $E^-_0 \simeq \frac{1}{2}E^{xx}_{b,-}$. The dependence of squeezing on the driving power is shown in Fig. 3(c) at the optimal cavity and driving frequencies. Figure 3(d) shows the squeezing as a function of homodyne detection frequency, demonstrating a bandwidth of several meV. This large bandwidth stems from the cavity out-coupling rate [103] γ^p and exciton dephasing γ^x which are also in the meV range [93].

The input power of 1–10 mW is an order of magnitude below the typical range of 50–100 mW required to generate comparable squeezing levels in state-of-the-art on-chip devices with conventional third-order nonlinear media [26,28]. Specifically, in Ref. [104], squeezing in an optimized Si_3N_4 microring resonator is predicted down to 84% (−0.75 dB) for a driving power of 10 mW, whereas we predict 33% (−4.8 dB) for the same power.

To understand the dominating physical processes responsible for squeezing, we show in Fig. 4 the squeezing as a function of drive frequency along with the three contributions to the parametric gain $\mathbf{\Delta}$ from Eq. (3). The cavity detuning has been chosen by numerically optimizing the

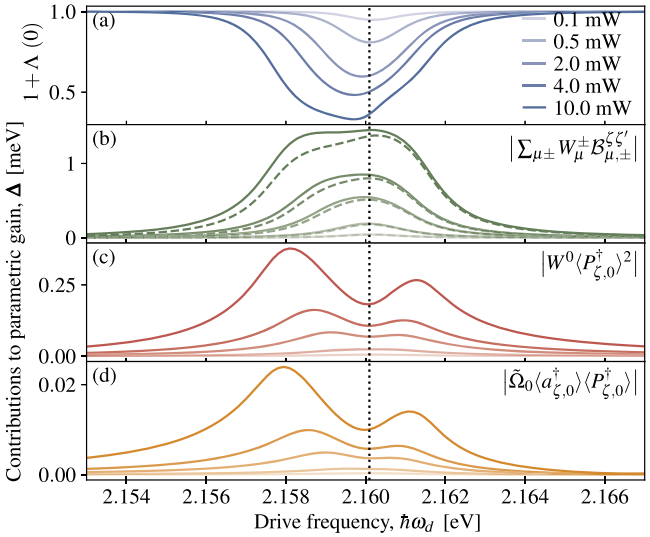

FIG. 4. (a) Copolarized squeezing versus driving frequency for optimized cavity detuning at different driving power levels. (b)–(d) Contributions to parametric gain from biexcitonic correlations (b), mean-field Coulomb interaction (c), and Pauli blocking (d). The contributions in (c) and (d) only have diagonal contributions in the ζ basis, which are equal for linearly polarized driving. In (b) the diagonal and off-diagonal contributions have been added. The dashed lines in (b) show the contribution from the bound biexciton alone ($\mu = b$, strictly off diagonal). The vertical dotted line indicates the two-photon resonance $\frac{1}{2} E^{xx}_{b,-}$.

squeezing as in Fig. 3. The contribution from exciton-photon correlations $\mathcal{C}^{\zeta\zeta'}_{\mathbf{q}}$ was found to be negligible and is not shown here. The contributions from biexcitonic correlations exceed the mean-field Coulomb and Pauli blocking by almost an order of magnitude. We can single out the contribution from the bound biexciton ($\mu = b$) in Eq. (3) [dashed lines in Fig. 4(b)], which accounts for more than 80% of the total parametric gain in the frequency region with strongest squeezing. Thus, resonant Coulomb-mediated biexciton formation as shown in Figs. 1(c) and 1(d) is the main contribution to the parametric gain and squeezing.

Conclusion.—In conclusion, we have presented a theoretical analysis of the generation of quadrature-squeezed light using the biexcitonic resonance in an atomically thin semiconductor coupled to an optical microcavity. We have shown that significant levels of broadband squeezing can be generated with very low input power levels of the order of 1–10 mW.

A previous experimental investigation [38] measured parametric gain from biexcitons in a bulk CuCl microcavity in the near-uv spectral range. The squeezing level at pump power equivalent to 63 mW for the spot size considered here was inferred to 0.63% (−2 dB), although not directly measured. Furthermore, we note that ZnO quantum wells with biexciton binding energies around 15 meV [105] are another interesting platform to potentially observe the predicted squeezing mechanism in the near-uv spectrum.

An interesting extension of the use of atomically thin semiconductors for quadrature squeezing is to introduce an electromagnetic nanoresonator with tight in-plane optical confinement [106–113]. Such structures could potentially enhance the efficiency, because the in-plane confinement leads to a stronger nonlinear response [114,115].

We thank Erik Bærentsen and Malte Selig for insightful discussions. E. V. D. acknowledges support from Independent Research Fund Denmark through an International Postdoc Fellowship (Grant No. 0164-00014B). F. K. and A. K. gratefully acknowledge support from the Deutsche Forschungsgemeinschaft through Projects No. 420760124 (KN 427/11-1) and No. 163436311—SFB 910 (Project B1).

[1] C. M. Caves, Phys. Rev. D **23**, 1693 (1981).
[2] M. A. Taylor, J. Janousek, V. Daria, J. Knittel, B. Hage, H.-A. Bachor, and W. P. Bowen, Nat. Photonics **7**, 229 (2013).
[3] J. Aasi, J. Abadie, B. P. Abbott, R. Abbott, T. D. Abbott, M. R. Abernathy, C. Adams, T. Adams, P. Addesso, R. X. Adhikari *et al.*, Nat. Photonics **7**, 613 (2013).
[4] S. Lloyd and S. L. Braunstein, *Quantum Information with Continuous Variables* (Springer, Berlin, 1999), pp. 9–17.
[5] N. J. Cerf, M. Levy, and G. Van Assche, Phys. Rev. A **63**, 052311 (2001).
[6] N. C. Menicucci, P. van Loock, M. Gu, C. Weedbrook, T. C. Ralph, and M. A. Nielsen, Phys. Rev. Lett. **97**, 110501 (2006).
[7] N. C. Menicucci, Phys. Rev. Lett. **112**, 120504 (2014).
[8] M. Hillery, Phys. Rev. A **61**, 022309 (2000).
[9] J. Huh, G. G. Guerreschi, B. Peropadre, J. R. McClean, and A. Aspuru-Guzik, Nat. Photonics **9**, 615 (2015).
[10] C. Sparrow, E. Martín-López, N. Maraviglia, A. Neville, C. Harrold, J. Carolan, Y. N. Joglekar, T. Hashimoto, N. Matsuda, J. L. O'Brien, D. P. Tew, and A. Laing, Nature (London) **557**, 660 (2018).
[11] L. Banchi, M. Fingerhuth, T. Babej, C. Ing, and J. M. Arrazola, Sci. Adv. **6**, eaax1950 (2020).
[12] R. E. Slusher, L. W. Hollberg, B. Yurke, J. C. Mertz, and J. F. Valley, Phys. Rev. Lett. **55**, 2409 (1985).
[13] L.-A. Wu, H. J. Kimble, J. L. Hall, and H. Wu, Phys. Rev. Lett. **57**, 2520 (1986).
[14] G. Breitenbach, S. Schiller, and J. Mlynek, Nature (London) **387**, 471 (1997).
[15] H. Vahlbruch, M. Mehmet, S. Chelkowski, B. Hage, A. Franzen, N. Lastzka, S. Gossler, K. Danzmann, and R. Schnabel, Phys. Rev. Lett. **100**, 033602 (2008).
[16] H. Vahlbruch, M. Mehmet, K. Danzmann, and R. Schnabel, Phys. Rev. Lett. **117**, 110801 (2016).
[17] J. U. Fürst, D. V. Strekalov, D. Elser, A. Aiello, U. L. Andersen, C. Marquardt, and G. Leuchs, Phys. Rev. Lett. **106**, 113901 (2011).
[18] G. Harder, T. J. Bartley, A. E. Lita, S. W. Nam, T. Gerrits, and C. Silberhorn, Phys. Rev. Lett. **116**, 143601 (2016).
[19] F. Lenzini, J. Janousek, O. Thearle, M. Villa, B. Haylock, S. Kasture, L. Cui, H.-P. Phan, D. V. Dao, H. Yonezawa, P. K. Lam, E. H. Huntington, and M. Lobino, Sci. Adv. **4**, eaat9331 (2018).

[20] A. Otterpohl, F. Sedlmeir, U. Vogl, T. Dirmeier, G. Shafiee, G. Schunk, D. V. Strekalov, H. G. Schwefel, T. Gehring, U. L. Andersen, G. Leuchs, and C. Marquardt, Optica **6**, 1375 (2019).

[21] R. M. Shelby, M. D. Levenson, S. H. Perlmutter, R. G. DeVoe, and D. F. Walls, Phys. Rev. Lett. **57**, 691 (1986).

[22] M. Rosenbluh and R. M. Shelby, Phys. Rev. Lett. **66**, 153 (1991).

[23] K. Bergman and H. A. Haus, Opt. Lett. **16**, 663 (1991).

[24] M. A. Finger, T. S. Iskhakov, N. Y. Joly, M. V. Chekhova, and P. S. J. Russell, Phys. Rev. Lett. **115**, 143602 (2015).

[25] A. Dutt, K. Luke, S. Manipatruni, A. L. Gaeta, P. Nussenzveig, and M. Lipson, Phys. Rev. Applied **3**, 044005 (2015).

[26] Y. Zhao, Y. Okawachi, J. K. Jang, X. Ji, M. Lipson, and A. L. Gaeta, Phys. Rev. Lett. **124**, 193601 (2020).

[27] V. D. Vaidya, B. Morrison, L. G. Helt, R. Shahrokshahi, D. H. Mahler, M. J. Collins, K. Tan, J. Lavoie, A. Repingon, M. Menotti, N. Quesada, R. C. Pooser, A. E. Lita, T. Gerrits, S. W. Nam, and Z. Vernon, Sci. Adv. **6**, eaba9186 (2020).

[28] Y. Zhang, M. Menotti, K. Tan, V. D. Vaidya, D. H. Mahler, L. G. Helt, L. Zatti, M. Liscidini, B. Morrison, and Z. Vernon, Nat. Commun. **12**, 2233 (2021).

[29] C. H. Schulte, J. Hansom, A. E. Jones, C. Matthiesen, C. Le Gall, and M. Atatüre, Nature (London) **525**, 222 (2015).

[30] A. M. Fox, J. J. Baumberg, M. Dabbicco, B. Huttner, and J. F. Ryan, Phys. Rev. Lett. **74**, 1728 (1995).

[31] J. P. Karr, A. Baas, R. Houdré, and E. Giacobino, Phys. Rev. A **69**, 031802(R) (2004).

[32] T. Boulier, M. Bamba, A. Amo, C. Adrados, A. Lemaitre, E. Galopin, I. Sagnes, J. Bloch, C. Ciuti, E. Giacobino, and A. Bramati, Nat. Commun. **5**, 3260 (2014).

[33] U. L. Andersen, T. Gehring, C. Marquardt, and G. Leuchs, Phys. Scr. **91**, 053001 (2016).

[34] C. Gardiner and P. Zoller, *Quantum Noise: A Handbook of Markovian and Non-Markovian Quantum Stochastic Methods with Applications to Quantum Optics* (Springer, Berlin, 2004).

[35] D. J. Lovering, R. T. Phillips, G. J. Denton, and G. W. Smith, Phys. Rev. Lett. **68**, 1880 (1992).

[36] K. Brunner, G. Abstreiter, G. Böhm, G. Tränkle, and G. Weimann, Phys. Rev. Lett. **73**, 1138 (1994).

[37] A. R. Hassan, Physica Status Solidi (b) **181**, 233 (1994).

[38] R. Shimano, Y. P. Svirko, A. Mysyrowicz, and M. Kuwata-Gonokami, Phys. Rev. Lett. **89**, 233601 (2002).

[39] V. Shahnazaryan, I. Iorsh, I. A. Shelykh, and O. Kyriienko, Phys. Rev. B **96**, 115409 (2017).

[40] F. Katsch, M. Selig, A. Carmele, and A. Knorr, Physica Status Solidi (b) **255**, 1800185 (2018).

[41] P. Stepanov, A. Vashisht, M. Klaas, N. Lundt, S. Tongay, M. Blei, S. Höfling, T. Volz, A. Minguzzi, J. Renard, C. Schneider, and M. Richard, Phys. Rev. Lett. **126**, 167401 (2021).

[42] Y. You, X.-X. Zhang, T. C. Berkelbach, M. S. Hybertsen, D. R. Reichman, and T. F. Heinz, Nat. Phys. **11**, 477 (2015).

[43] A. Steinhoff, M. Florian, and F. Jahnke, Phys. Rev. B **101**, 045411 (2020).

[44] S. Latini, T. Olsen, and K. S. Thygesen, Phys. Rev. B **92**, 245123 (2015).

[45] X. Liu, T. Galfsky, Z. Sun, F. Xia, E.-c. Lin, Y.-H. Lee, S. Kéna-Cohen, and V. M. Menon, Nat. Photonics **9**, 30 (2015).

[46] S. Dufferwiel, S. Schwarz, F. Withers, A. A. P. Trichet, F. Li, M. Sich, O. Del Pozo-Zamudio, C. Clark, A. Nalitov, D. D. Solnyshkov, G. Malpuech, K. S. Novoselov, J. M. Smith, M. S. Skolnick, D. N. Krizhanovskii, and A. I. Tartakovskii, Nat. Commun. **6**, 8579 (2015).

[47] M. Sidler, P. Back, O. Cotlet, A. Srivastava, T. Fink, M. Kroner, E. Demler, and A. Imamoglu, Nat. Phys. **13**, 255 (2017).

[48] C. Anton-Solanas, M. Waldherr, M. Klaas, H. Suchomel, T. H. Harder, H. Cai, E. Sedov, S. Klembt, A. V. Kavokin, S. Tongay, K. Watanabe, T. Taniguchi, S. Höfling, and C. Schneider, Nat. Mater. **20**, 1233 (2021).

[49] M. Collett, R. Loudon, and C. Gardiner, J. Mod. Opt. **34**, 881 (1987).

[50] H. J. Carmichael, J. Opt. Soc. Am. B **4**, 1588 (1987).

[51] V. M. Axt and A. Stahl, Z. Phys. B Condens. Matter **93**, 195 (1994).

[52] M. Lindberg, Y. Z. Hu, R. Binder, and S. W. Koch, Phys. Rev. B **50**, 18060 (1994).

[53] T. Östreich, K. Schönhammer, and L. J. Sham, Phys. Rev. Lett. **74**, 4698 (1995).

[54] W. Schäfer, D. S. Kim, J. Shah, T. C. Damen, J. E. Cunningham, K. W. Goossen, L. N. Pfeiffer, and K. Köhler, Phys. Rev. B **53**, 16429 (1996).

[55] S. Savasta and R. Girlanda, Phys. Rev. Lett. **77**, 4736 (1996).

[56] S. Savasta and R. Girlanda, Phys. Rev. B **59**, 15409 (1999).

[57] M. Kira, F. Jahnke, W. Hoyer, and S. W. Koch, Prog. Quantum Electron. **23**, 189 (1999).

[58] N. H. Kwong, R. Takayama, I. Rumyantsev, M. Kuwata-Gonokami, and R. Binder, Phys. Rev. B **64**, 045316 (2001).

[59] R. Takayama, N. H. Kwong, I. Rumyantsev, M. Kuwata-Gonokami, and R. Binder, Eur. Phys. J. B **25**, 445 (2002).

[60] S. Savasta, O. Di Stefano, and R. Girlanda, Phys. Rev. Lett. **90**, 096403 (2003).

[61] S. Schumacher, G. Czycholl, F. Jahnke, I. Kudyk, L. Wischmeier, I. Rückmann, T. Voss, J. Gutowski, A. Gust, and D. Hommel, Phys. Rev. B **72**, 081308(R) (2005).

[62] S. Schumacher, G. Czycholl, and F. Jahnke, Phys. Rev. B **73**, 035318 (2006).

[63] S. Portolan, O. Di Stefano, S. Savasta, F. Rossi, and R. Girlanda, Phys. Rev. B **77**, 195305 (2008).

[64] F. Katsch, M. Selig, and A. Knorr, 2D Mater. **7**, 015021 (2020).

[65] F. Katsch, M. Selig, and A. Knorr, Phys. Rev. Lett. **124**, 257402 (2020).

[66] F. Katsch and A. Knorr, Phys. Rev. X **10**, 041039 (2020).

[67] H. Eleuch, J. M. Courty, G. Messin, C. Fabre, and E. Giacobino, J. Opt. B **1**, 1 (1999).

[68] G. Messin, J. P. Karr, H. Eleuch, J. M. Courty, and E. Giacobino, J. Phys. Condens. Matter **11**, 6069 (1999).

[69] P. Schwendimann, C. Ciuti, and A. Quattropani, Phys. Rev. B **68**, 165324 (2003).

[70] A. Quattropani and P. Schwendimann, Physica Status Solidi (b) **242**, 2302 (2005).
[71] M. Romanelli, J. P. Karr, C. Leyder, E. Giacobino, and A. Bramati, Phys. Rev. B **82**, 155313 (2010).
[72] H. Oka and H. Ajiki, Phys. Rev. B **83**, 045305 (2011).
[73] See Supplemental Material at http://link.aps.org/supplemental/10.1103/PhysRevLett.129.097401 for for derivations of the equations in the main text and details of the numerical calculations, which includes Refs. [74–80].
[74] A. L. Ivanov and H. Haug, Phys. Rev. B **48**, 1490 (1993).
[75] M. Florian, M. Hartmann, A. Steinhoff, J. Klein, A. W. Holleitner, J. J. Finley, T. O. Wehling, M. Kaniber, and C. Gies, Nano Lett. **18**, 2725 (2018).
[76] N.-H. Kwong, J. R. Schaibley, and R. Binder, Phys. Rev. B **104**, 245434 (2021).
[77] A. P. Rooney, A. Kozikov, A. N. Rudenko, E. Prestat, M. J. Hamer, F. Withers, Y. Cao, K. S. Novoselov, M. I. Katsnelson, R. Gorbachev, and S. J. Haigh, Nano Lett. **17**, 5222 (2017).
[78] F. A. Rasmussen and K. S. Thygesen, J. Phys. Chem. C **119**, 13169 (2015).
[79] A. Kormányos, G. Burkard, M. Gmitra, J. Fabian, V. Zólyomi, N. D. Drummond, and V. Fal'ko, 2D Mater. **2**, 022001 (2015).
[80] A. Kumar and P. K. Ahluwalia, Physica (Amsterdam) **407B**, 4627 (2012).
[81] K. F. Mak, C. Lee, J. Hone, J. Shan, and T. F. Heinz, Phys. Rev. Lett. **105**, 136805 (2010).
[82] A. Splendiani, L. Sun, Y. Zhang, T. Li, J. Kim, C.-Y. Chim, G. Galli, and F. Wang, Nano Lett. **10**, 1271 (2010).
[83] A. Kuc, N. Zibouche, and T. Heine, Phys. Rev. B **83**, 245213 (2011).
[84] D. Xiao, G.-B. Liu, W. Feng, X. Xu, and W. Yao, Phys. Rev. Lett. **108**, 196802 (2012).
[85] T. Cao, G. Wang, W. Han, H. Ye, C. Zhu, J. Shi, Q. Niu, P. Tan, E. Wang, B. Liu, and L. Feng, Nat. Commun. **3**, 887 (2012).
[86] M. S. Skolnick, T. A. Fisher, and D. M. Whittaker, Semicond. Sci. Technol. **13**, 645 (1998).
[87] R. Osgood Jr and X. Meng, *Principles of Photonic Integrated Circuits* (Springer, Berlin, 2021), pp. 31–55.
[88] G. H. Wannier, Phys. Rev. **52**, 191 (1937).
[89] L. J. Sham and T. M. Rice, Phys. Rev. **144**, 708 (1966).
[90] M. Kira and S. W. Koch, Prog. Quantum Electron. **30**, 155 (2006).
[91] A. Ramasubramaniam, Phys. Rev. B **86**, 115409 (2012).
[92] W. Schäfer and M. Wegener, *Semiconductor Optics and Transport Phenomena* (Springer, Berlin, 2013).
[93] M. Selig, G. Berghäuser, A. Raja, P. Nagler, C. Schüller, T. F. Heinz, T. Korn, A. Chernikov, E. Malic, and A. Knorr, Nat. Commun. **7**, 13279 (2016).
[94] D. Christiansen, M. Selig, G. Berghäuser, R. Schmidt, I. Niehues, R. Schneider, A. Arora, S. M. de Vasconcellos, R. Bratschitsch, E. Malic, and A. Knorr, Phys. Rev. Lett. **119**, 187402 (2017).
[95] Z. Khatibi, M. Feierabend, M. Selig, S. Brem, C. Linderälv, P. Erhart, and E. Malic, 2D Mater. **6**, 015015 (2018).
[96] S. Brem, J. Zipfel, M. Selig, A. Raja, L. Waldecker, J. D. Ziegler, T. Taniguchi, K. Watanabe, A. Chernikov, and E. Malic, Nanoscale **11**, 12381 (2019).
[97] F. Lengers, T. Kuhn, and D. E. Reiter, Phys. Rev. B **101**, 155304 (2020).
[98] C. Sieh, T. Meier, F. Jahnke, A. Knorr, S. W. Koch, P. Brick, M. Hübner, C. Ell, J. Prineas, G. Khitrova, and H. M. Gibbs, Phys. Rev. Lett. **82**, 3112 (1999).
[99] D. A. Steck, Quantum and atom optics, http://steck.us/teaching (revision 0.13.10, 2021).
[100] M. Lax, Phys. Rev. **145**, 110 (1966).
[101] S. Franke, S. Hughes, M. K. Dezfouli, P. T. Kristensen, K. Busch, A. Knorr, and M. Richter, Phys. Rev. Lett. **122**, 213901 (2019).
[102] S. Portolan, O. Di Stefano, S. Savasta, F. Rossi, and R. Girlanda, Phys. Rev. B **77**, 035433 (2008).
[103] U. B. Hoff, B. M. Nielsen, and U. L. Andersen, Opt. Express **23**, 12013 (2015).
[104] H. Seifoory, Z. Vernon, D. H. Mahler, M. Menotti, Y. Zhang, and J. E. Sipe, Phys. Rev. A **105**, 033524 (2022).
[105] H. J. Ko, Y. F. Chen, T. Yao, K. Miyajima, A. Yamamoto, and T. Goto, Appl. Phys. Lett. **77**, 537 (2000).
[106] J. Wen, H. Wang, W. Wang, Z. Deng, C. Zhuang, Y. Zhang, F. Liu, J. She, J. Chen, H. Chen, S. Deng, and N. Xu, Nano Lett. **17**, 4689 (2017).
[107] D. Zheng, S. Zhang, Q. Deng, M. Kang, P. Nordlander, and H. Xu, Nano Lett. **17**, 3809 (2017).
[108] M.-E. Kleemann, R. Chikkaraddy, E. M. Alexeev, D. Kos, C. Carnegie, W. Deacon, A. C. De Pury, C. Große, B. De Nijs, J. Mertens, A. I. Tartakovskii, and J. J. Baumberg, Nat. Commun. **8**, 1296 (2017).
[109] J. Cuadra, D. G. Baranov, M. Wersäll, R. Verre, T. J. Antosiewicz, and T. Shegai, Nano Lett. **18**, 1777 (2018).
[110] M. Stührenberg, B. Munkhbat, D. G. Baranov, J. Cuadra, A. B. Yankovich, T. J. Antosiewicz, E. Olsson, and T. Shegai, Nano Lett. **18**, 5938 (2018).
[111] X. Han, K. Wang, X. Xing, M. Wang, and P. Lu, ACS Photonics **5**, 3970 (2018).
[112] M. Geisler, X. Cui, J. Wang, T. Rindzevicius, L. Gammelgaard, B. S. Jessen, P. A. D. Goncalves, F. Todisco, P. Bøggild, A. Boisen, M. Wubs, N. A. Mortensen, S. Xiao, and N. Stenger, ACS Photonics **6**, 994 (2019).
[113] J. Qin, Y.-H. Chen, Z. Zhang, Y. Zhang, R. J. Blaikie, B. Ding, and M. Qiu, Phys. Rev. Lett. **124**, 063902 (2020).
[114] E. V. Denning, M. Wubs, N. Stenger, J. Mørk, and P. T. Kristensen, Phys. Rev. B **105**, 085306 (2022).
[115] E. V. Denning, M. Wubs, N. Stenger, J. Mørk, and P. T. Kristensen, Phys. Rev. Research **4**, L012020 (2022).